DE GRUYTER Energy Harvesting and Systems 2015; 2(3-4): 107–112

Xinyun Gu, Ying Yang*, Ji Chen and Yiping Wang

Temperature-Dependent Properties of a 1–3 Connectivity Piezoelectric Ceramic–Polymer Composite

Abstract: In this work, the 1–3 connectivity piezoelectric ceramic–polymer composites have been fabricated by a viscous-polymer processing, where $0.90Pb(Zr_{0.52}Ti_{0.48})O_3$–$0.05Pb(Mn_{1/3}Sb_{2/3})O_3$–$0.05Pb(Zn_{1/3}Nb_{2/3})O_3$ (PZT–PMS–PZN) fibers with 0.5 volume fraction were aligned in epoxy matrix. The sintered PZT fibers, with average diameter of 300 µm and aspect ratio (height/diameter) higher than 3, all showed a pure perovskite phase structure and highly dense morphology. The dielectric, piezoelectric, ferroelectric properties and the vibration modes of the 1–3 composites were measured and demonstrated in comparison with that of the monolithic piezoelectric ceramics. The results confirmed that the 1–3 composites possessed a low acoustic impedance (Z) of 13 MRayl and a high thickness coupling coefficient (k_t) of 0.59, in addition, only single thickness vibration mode with the resonance frequency over 1.5 MHz was observed. With temperature elevation, the properties including dielectric constant ε_r, k_t, the ratio of k_t to k_p (k_t/k_p) and the acoustic impedance (Z) increase, while the planar electromechanical coupling coefficient (k_p) show opposite temperature dependence. Under test temperature of 100°C, the 1–3 composites still present excellent temperature stability with increased k_t/k_p ratio up to 3.6. The researches on temperature-dependent properties of the 1–3 composites are critical for improving its applications in various environments.

Keywords: 1–3 composites, piezoelectric properties, dielectric properties, PZT

DOI 10.1515/ehs-2014-0049

Introduction

1–3 connectivity piezoelectric ceramic–polymer composites have been widely used for piezoelectric transducers in many fields, such as hydrophones for low-frequency (Zhang et al. 1993), ultrasonic transducers (Chen et al. 2013), non-destructive testing for high frequency (Kirk and Schmarje 2013) and so on. Comparing with monolithic $0.90Pb(Zr_{0.52}Ti_{0.48})O_3$ (PZT) ceramics, the 1–3 composites show advantages of higher piezoelectric constants g_h, higher value of k_t, flexible processing in manufacturing, and relatively low impendence Z which leads to better material performance in matching with human tissue and water (Dyaz and Castillero 2001; Wang et al. 2008). At present, methods developed for processing fine-scale 1–3 piezoelectric composites include dice-and-fill (Xu et al. 2012), injection molding (Leslie, Gentilman, and Pham 1993), viscous-polymer processing (VPP) (Abrar et al. 2004; Bernassau et al. 2012), among which dice-and-fill is the uppermost process because of its mature technique and easy setup preparation. On the other hand, in the VPP, the size and shape of fibers can be changed flexibly as well as the distribution in the composites, therefore the prepared 1–3 composites have advantages in optimizing the material properties to meet various requirements for different applications (Bowen and Stevens 2006). Now there are many studies (Zhen and Li 2008; Zhou et al. 2011; Shen, Xu, and Li 2009; Chaipanich et al. 2011; Potong et al. 2012; Ramesh et al. 2011) focusing on the 1–3 composites, mostly concentrating on the preparation, the dielectric and ferroelectric properties at room temperature. The material properties of 1–3 composites are decisively determined by the piezoelectric phase and the polymer matrix. However, comparing with the piezoelectric phase, the epoxy matrix is

---

***Corresponding author: Ying Yang,** State Key Laboratory of Mechanics and Control of Mechanical Structures, Nanjing University of Aeronautics and Astronautics, Nanjing 210016, China, E-mail: yingyang@nuaa.edu.cn
Xinyun Gu, State Key Laboratory of Mechanics and Control of Mechanical Structures, Nanjing University of Aeronautics and Astronautics, Nanjing 210016, China; College of Materials Science and Technology, Nanjing University of Aeronautics and Astronautics, Nanjing 210016, China; Patent Examination Cooperation Jiangsu Center of the Patent Office, SIPO, Suzhou, Jiangsu Sheng, China
Ji Chen, State Key Laboratory of Mechanics and Control of Mechanical Structures, Nanjing University of Aeronautics and Astronautics, Nanjing 210016, China; College of Materials Science and Technology, Nanjing University of Aeronautics and Astronautics, Nanjing 210016, China
Yiping Wang, State Key Laboratory of Mechanics and Control of Mechanical Structures, Nanjing University of Aeronautics and Astronautics, Nanjing 210016, China

much more sensitive to temperature for the creeping behavior of the molecular chain and the segment of the epoxy at high temperature, which makes the epoxy phase temperature sensitive with poor heating stability (Majda and Skrodzewicz 2009). Transducers or sensors containing the 1–3 composites are always served at different or even extreme environment with varying temperatures, so it is quite important and necessary to study the temperature dependent properties of the 1–3 composites. However, the performance of the 1–3 composites concerning the temperature changing has not been researched sufficiently. In this study, temperature dependences of the vibration mode, dielectric properties, piezoelectric properties, ferroelectric hysteresis behavior of the 1–3 connectivity PZT composites are investigated.

Experiment

The piezoelectric fibers of $0.90Pb(Zr_{0.52}Ti_{0.48})O_3$–$0.05Pb(Mn_{1/3}Sb_{2/3})O_3$–$0.05Pb(Zn_{1/3}Nb_{2/3})O_3$ (abbreviated as PZT–PMS–PZN) were prepared by VPP, including the preparation of PZT powder, and a sintering process at 1,100°C for 3 h. The diameter of a single sintered piezoelectric fiber is about 300 μm. The piezoelectric fibers were aligned vertically in a sample holder, followed by casting low viscosity epoxy to form a fiber/epoxy 1–3 composite, where the epoxy was firstly degassed for 30 min and then cured at 80°C for 4 h. The composite was then cut into thin disk and painted with low-temperature silver paste on both sides. The thickness of the 1–3 composite sample is 1 mm and the volume fraction of the piezoelectric fibers (φ) is about 50%. The composite samples were then poled at 80°C for 30 min under an applied field of 40 kV/cm in silicone oil.

The density of the 1–3 composites was measured by Archimedes method with an average value of 4.38 g/cm^3. The crystal structure of the piezoelectric fibers was examined using an X-ray diffractometer (XRD, Bruker D8 Advanced, CuKα radiation, $\lambda = 0.15418$ nm). The microstructures of the piezoelectric fibers were observed by a scanning electrical microscopy (SEM, Leo 1550, Zeiss Company). The piezoelectric coefficient (d_{33}) was measured using a quasi-static piezo-d_{33} meter (ZJ-3A, Institute of Acoustics Academia Sinica) after aging the samples for 24 h. All the temperature-dependent properties such as dielectric permittivityε_r, the planar coupling coefficient (k_p), the thickness coupling coefficient (k_t), acoustic velocity (υ_L) and the acoustic impedance (Z) were measured by using an impedance analyzer (Agilent 4294A) in a temperature control system (Linkam), where the values of k_p, k_t and the mechanical quality factor (Q_m) were determined from the resonance and antiresonance method based on the IEEE standards. The dielectric permittivity ε_{33}^T determined by measuring the capacitance C at 1 kHz was then calculated from the equation:

$$\varepsilon_{33}^T = \frac{Ct}{\varepsilon_0 S} \quad [1]$$

where S is the electrode area and t is the thickness of the sample, and ε_0 is the permittivity of the free space. The sound velocity υ_L and acoustic impedance Z were calculated from the following formulas:

$$\upsilon_L = 2tf_a \quad [2]$$

$$Z = \rho \upsilon_L \quad [3]$$

where t, f_a and ρ are the thickness, antiresonant frequency and density of the sample, respectively. Ferroelectric hysteresis loops were measured under 35 kV/cm electric field at room temperature by using a ferro-analyzer (TF2000, aixACCT GmbH).

Results and Discussions

The typical piezoelectric properties for the 1–3 composite and piezoelectric ceramic are listed in Table 1. The data comparison displays that PZT ceramic has a much larger value of ε_{33}^T, Q_m, $d_{33,}$ Z, k_p, and a relatively smaller value of $\tan\delta$, k_t. The 1–3 composites usually work in thickness mode, so the dynamic properties such as electromechanical coupling coefficient k_t, mechanical quality factor Q_m and the ratio of k_t to k_p were significantly determined by the resonant f_r and antiresonant frequencies f_a at thickness resonance mode. Usually, for piezoelectric material,

Table 1: Material parameters of the 1–3 composite and PZT ceramic determined by normalized spectrum method and IEEE standard method at room temperature.

	PZT ceramic	1–3 composite
Dielectric permittivity (ε_{33}^T)	1,400	612
Acoustic impedance (Z)	34	13.5
Planar coupling coefficient (k_p)	0.59	0.28
Thickness coupling coefficient (k_t)	0.47	0.59
The ratio of k_t to k_p (k_t/k_p)	0.80	2.1
Mechanical quality (Q_m)	1,500	9.9
Dielectric loss $\tan\delta$(%)	0.35	0.54
Peizoelectric strain constant (d_{33})	350	300

higher thickness coupling coefficient k_t means higher power transduction capability. For 1–3 composites, a larger k_t/k_p value is necessary for better resolution in anisotropy. From Table 1, the k_t of the 1–3 composite is 0.59 and the k_t/k_p value is 2.1, showing a clear thickness mode. Moreover, another typical dynamic property for the 1–3 composite is the mechanical quality factor Q_m (about 10), which is beneficial to application in the imaging transducers for the characteristic of obtaining broad operating bandwidth (Lee et al. 2012). Besides, the acoustic impendence Z of the 1–3 composites is also much lower than PZT ceramics because of the lower acoustic impendence of polymer, therefore the 1–3 composites are more suitable for applications requiring good matching with human tissue and water. In all, the special characteristics of the 1–3 composites in high quality ensure the wide applications in many fields.

Figure 1(a) depicts the XRD patterns of PZT–PMS–PZN fibers in 2θ range between 20° and 60°. It can be seen that the specimen exhibits a pure perovskite structure; no discernible peaks of second phases such as pyrochlore is observed, indicating that the adding organics do not affect the forming of the perovskite structure. Figure 1(b) shows the SEM micrograph for the cross section of the sintered piezoelectric fibers with a high-density morphology and the diameter of a single piezoelectric fiber is about 300 μm. Moreover, Figure 1(c) shows the SEM micrograph of inner grains of piezoelectric fiber with the average grain size around 2–4 μm.

Figure 2(a) shows the contrast in the impedance characteristic of the 1–3 composite and the monolithic piezoelectric ceramic. As shown, the piezoelectric ceramic has two major resonance modes: planar mode and thickness mode, in which the planar mode is the typical working mode for monolithic piezoelectric ceramic. On the contrary, for the 1–3 composites, the low-frequency resonance at planar mode has been remarkably depressed and only the thickness resonance mode with resonance frequency over 1 MHz is seen. Figure 2(b) shows the trend about the impedance Z and phase

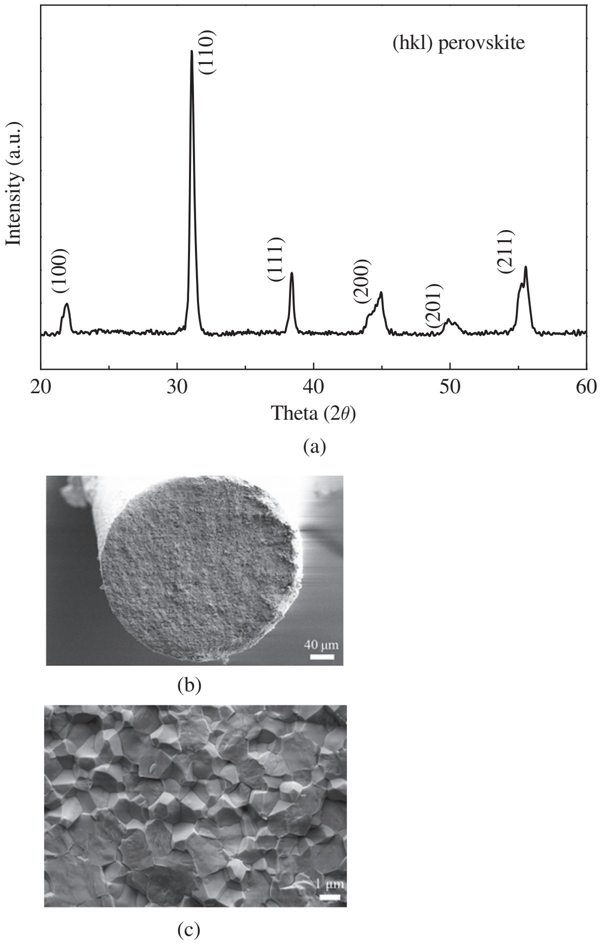

(a)

(b)

(c)

Figure 1: (a) XRD patterns of PZT–PMS–PZN fibers; (b) SEM micrograph for sectional piezoelectric fiber; and (c) SEM micrograph revealing inner grains of piezoelectric fiber.

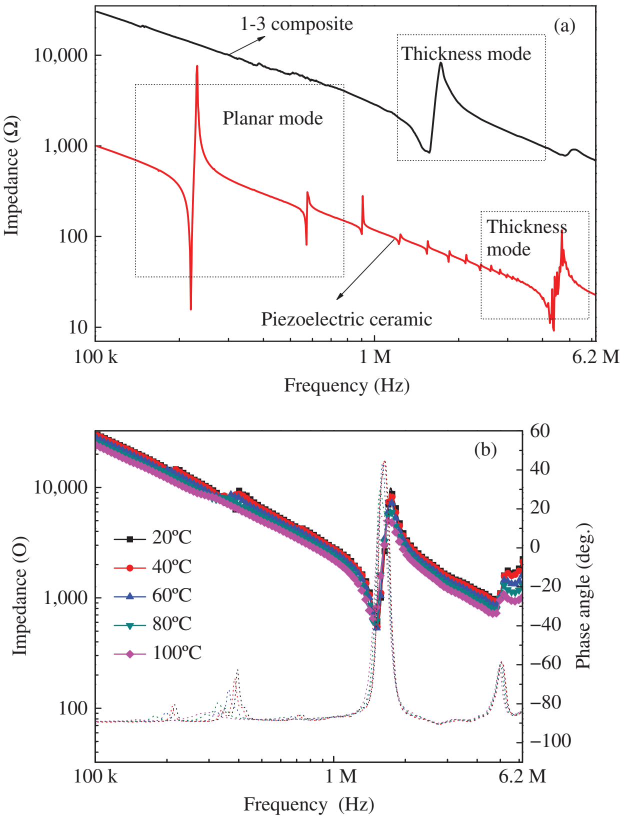

Figure 2: (a) Vibration mode comparison between the 1–3 composite and piezoelectric ceramic; (b) the temperature-dependent planar mode and thickness mode of the 1–3 composite with volume fraction $\phi = 50\%$.

angle of the 1–3 composite under various temperatures from 20°C to 100°C. From Figure 2(b), we can see that the antiresonant frequency fa and resonant frequency fr at the thickness mode and planar mode both decreased as temperature increases. Because of the temperature sensitivity of the epoxy phase, its elastic compliance increases distinctly when temperature increases. The 1–3 composite contains epoxy phase; thus, the overall elastic compliance shows increasing trend, resulting in decreased resonant frequency and antiresonant frequency correspondingly. However, the resonance peak at thickness mode is still clear even at the temperature of 100°C. In comparison, as to the planar mode, the resonance peak has been further depressed by rising temperature, and the major resonance peak almost disappeared at 100°C. Based on temperature-dependent vibrations at planar and thickness mode, this kind of 1–3 composites could work in the environment up to 100°C for the stable continuous vibration at thickness mode.

Figure 3 shows the temperature-dependent dielectric permittivity ε_r of the 1–3 composite at 1 kHz to 1 MHz from 30°C to 100°C. It can be seen that all the dielectric permittivity ε_r under different frequencies increase as temperature increases, and the dielectric permittivity ε_{33}^T value comes to 723 at 100°C, 1 kHz. In addition, the dielectric permittivity ε_r value decreases when the working frequency rises at a certain temperature, on the performance that ε_{33}^S is 676 at 100°C, 1 MHz. The ε_r value of the 1–3 piezoelectric composite is much lower than the piezoelectric ceramic due to the lower ε_r of the existing epoxy phase. However, the temperature dependence in dielectric permittivity ε_r of the 1–3 composite is in accordance with that of the piezoelectric ceramic, and adding of epoxy phase does not affect the typical regularity in dielectric permittivity of the piezoelectric composite materials. Meanwhile, the dielectric loss $\tan\delta$ shows the same trend with temperature as dielectric permittivity ε_r does. The dielectric loss of the 1–3 composite is higher than pure piezoelectric ceramic due to the contributions from the epoxy phase with a relatively high dielectric loss property.

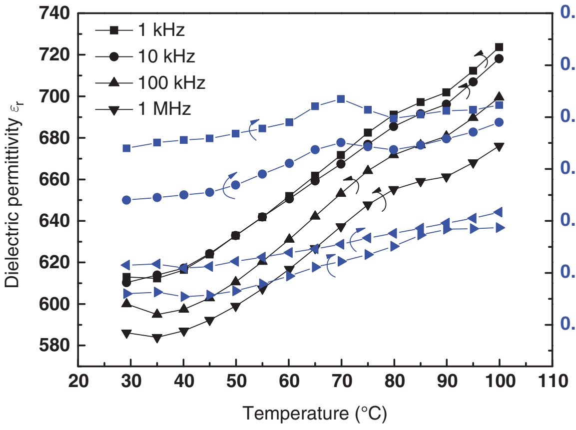

Figure 3: Temperature-dependent dielectric permittivity ε_r, dielectric loss $\tan\delta$ of the 1–3 composite at different frequencies.

Figure 4 shows the trend of the temperature-dependent k_p, k_t and k_t/k_p of the 1–3 composite with volume fraction ϕ of 50%. As observed from Figure 4, k_t increases with the temperature and reaches 0.705 at 100°C. On the contrary, the k_p value decreases as temperature increases and drops even faster at higher temperature. The k_p value decreased to almost 0 at 100°C, which is in accordance with Figure 1(b), showing that there is no obvious peak at planar mode. As a result, the k_t/k_p value increases all the time with the temperature. However, in this paper, temperature range is not wide enough considering the role of epoxy in the composite, and this kind of 1–3 composite shows the good characteristic of large k_t/k_p value within temperature of 100°C, which is an important factor to ensure the application of the 1–3 composite for its anisotropy property (Meryer, Lopath, and Yoshikawa 1997).

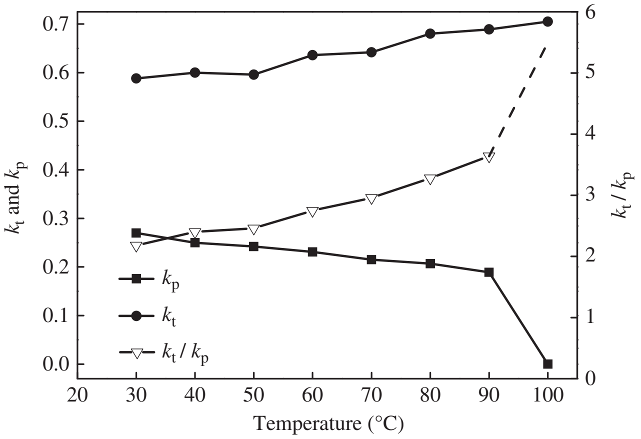

Figure 4: Temperature-dependent planar coupling coefficient k_p, thickness coupling coefficient (k_t), the ratio of k_t to k_p (k_t/k_p) of the 1–3 composite.

Figure 5 shows the temperature-dependent acoustic velocity υ_L and acoustic impedance Z of the 1–3 composite. From formulas about υ_L and Z (eq. [3]), it is known that the variation about the values of υ_L and Z shares a similar trend of f_a. From room temperature to 100°C, the average value of υ_L and Z is 3,018 m/s, 13.22 MRayl, respectively.

Figure 6 shows the P–E hysteresis loop which includes the contributions from PZT fibers and epoxy at room temperature. The extracted P–E loops of the 1–3

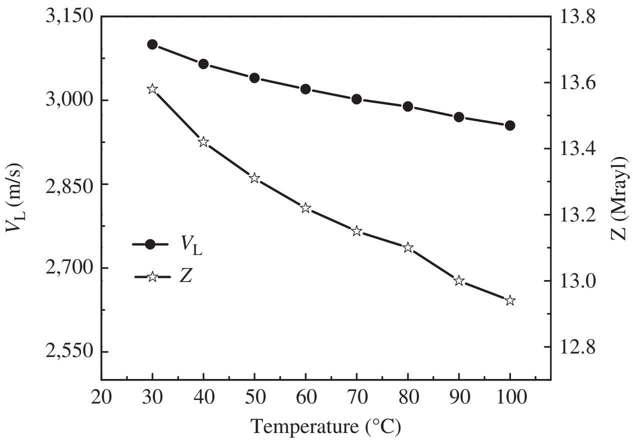

Figure 5: The temperature-dependent acoustic velocity v_L and acoustic impedance Z of the 1–3 composite.

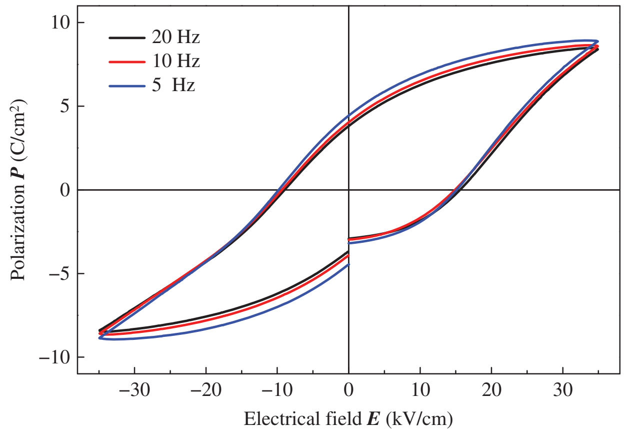

Figure 6: Ferroelectric polarization-electric field (*P–E*) hysteresis loops of the 1–3 composite at room temperature for different frequencies.

composite at different frequencies demonstrate a coercive field E_c of 9.83 kV/cm and a remnant polarization P_r of 4.42 μC/cm^2 at 5 Hz. At the frequency from 20 to 5 Hz, the P_r value is increased from 3.78 to 4.42 μC/cm^2, and the coercive field E_c increases from 8.96 to 9.83 kV/cm. Compared with the PZT bulk ceramic (E_c = 8.30 kV/cm, P_r = 7.80 μC/cm^2, 5 Hz), the coercive filed of the 1–3 composite is larger but the remnant polarization P_r is smaller. It is known that epoxy polymer is without ferroelectric polarization, so the role of epoxy decreases the total *P–E* effect of the 1–3 composite; therefore, the average value is smaller than the PZT bulk ceramics. Additionally, in the 1–3 composites, the high resistance of the polymer shields the external electric field, so the external electric field could not exert on the PZT fibers totally, which increases the coercive field and decreases the polarization as well (Sun et al. 2010).

Conclusions

The temperature-dependent dielectric, piezoelectric and ferroelectric properties of the 1–3 composites have been investigated in this study. The observed properties are critical for the application of the 1–3 composites in various environments, and the variation may be due to the temperature effects on the piezoelectric fibers and the epoxy matrix. A clear and uncoupled thickness mode is confirmed even at a high temperature of 100°C, indicating that there is a great potential for the composites to be applied in many circumstances.

Funding: This work was financially supported by the Natural Science Foundation of Jiangsu Province (no. BK2010504), the Doctoral Discipline Foundation of the Ministry of Education (no. 20103218120003) and NUAA research funding (no. NS2011006).

References

Abrar, A., D. Zhang, B. Su, and T. W. Button. 2004. “1–3 Connectivity Piezoelectric Ceramic-Polymer Composite Transducers Made with Viscous Polymer Processing for High Frequency Ultrasound.” *Ultrasonics* 42: 479–84.

Bernassau, A. L., G. G. Luis, D. Huston, et al. 2012. “Microfabrication of Electrode Patterns for High-Frequency Ultrasound Transducer Arrays.” *IEEE Transactions on Ultrasonics, Ferroelectrics and Frequency Control* 59: 1820–9.

Bowen, C. R., and R. Stevens. 2006. “Manufacture and Characterization of High Activity Piezoelectric Fibres.” *Smart Materials and Structures* 15: 295–301.

Chaipanich, A., R. Potong, R. Rianyoi, and L. Jareansuk. 2011. “Dielectric and Ferroelectric Hysteresis Properties of 1–3 Lead Magnesium Niobate-Lead Titante Ceramic/Portland Cement Composites.” *Ceramics International* 38: 255–8.

Chen, G. S., H. C. Liu, Y. C. Lin, et al. 2013. “Experimental Analysis of 1–3 Piezocomposites for High-Intensity Focused Ultrasound Transducer Applications.” *IEEE Transactions on Biomedical Engineering* 60: 128–34.

Dyaz, R. G., and J. B. Castillero. 2001. “Overall Properties of Piezocomposite Materials 1–3.” *Materials Letters* 48: 93–8.

Kirk, K. J., and N. Schmarje. 2013. “Experimental and Simulated Performance of Lithium Niobate 1–3 Piezocomposites for 2 MHz Non-Destructive Testing Applications.” *Ultrasonics* 53: 185–90.

Lee, H. J., S. J. Zhang, R. J. Meyer, et al. 2012. “Characterization of Piezoelectric Ceramics and 1–3 Composites for High Power Transducers.” *Applied Physics Letters* 101: 032902.

Leslie, J. B., L. R. Gentilman, and H. T. Pham. 1993. “Injection Mold Fine-Scale Piezoelectric Composite Transducers.” *IEEE Ultrasonics Symposium* 1–2: 499–503.

Majda, P., and J. Skrodzewicz. 2009. “A Modified Creep Model of Epoxy Adhesive at Ambient Temperature.” *International Journal of Adhesion and Adhesives* 29: 396–404.

Meryer, R. J., J. P. Lopath, and S. Yoshikawa. 1997. “High Frequency 1–3 Composite from Alkoxide-Derived PZT Fibers.”*IEEE Ultrasonics Symposium* 2: 915–18.

Potong, R., R. Rianyoi, N. Jaitanong, R. Yimnirun, et al. 2012. “Ferroelectric Hysteresis Behavior and Dielectric Properties of 1–3 Lead Zirconate Titanate–Cement Composites.” *Ceramics International* 38: 267–70.

Ramesh, R., S. Pereira, V. Kumar, et al. 2011. “Estimation of Certain Material Properties of a 1–3 Piezoelectric Composite as Functions of Temperature.” *Ferroelectronics* 423: 2–24.

Shen, Z. Y., Y. Xu, and J. F. Li. 2009. “Fabrication and Electromechanical Properties of Microscale 1–3-type Piezoelectric Composites Using (Na,K)NbO3-Based Pb-Free Piezoceramics.” *Journal of Applied Physics* 105: 104103.

Sun, C. L., L. F. Qin, H. Xue, et al. 2010. “Ferroelectric and Electromechanical Property Characterization of Single Pb(Z rTi) 03 Fiber Resonater.” *Journal of Applied Physics* 107: 024102.

Wang, L. K., L. Li, L. Qin, W. W. Wu, et al. 2008. “Study of Effective Properties of Modified 1–3 Piezocomposites.” *Journal of Applied Physics* 104: 064120.

Xu, Y., J. F. Li, J. Ma, et al. 2012. “Microscale 1–3-Type Lead-Free Piezoelectric/Ferrite Composites Fabricated by a Modified Dice-And-Fill Method.” *Journal of Physics D: Applied Physics* 45: 315306.

Zhang, Q. M., W. Cao, H. Wang, and L. E. Cross. 1993. “Characterization of the Performance of 1–3 Type Piezocomposites for Low-Frequency Applications.” *Journal of Applied Physics* 73: 1403–10.

Zhen, Y. H., and J. F. Li. 2008. “Preparation and Electrical Properties of Fine-Scale 1–3 Lead Zirconic Titanate/Epoxy Composite Thick Films for High-Frequency Ultrasonic Transducers.” *Journal of Applied Physics* 103: 084119.

Zhou, D., K. F. Cheung, K. H. Lam, et al. 2011. “Broad-Band and High-Temperature Ultrasonic Transducer Fabricated Using a Pb(In1/2Nb1/2)-Pb(Mg1/3Nb2/3)-PbTiO3 Single Crystal/Epoxy 1–3 Composite.” *Review of Scientific Instruments* 82: 055110–055110–7.